CHAPTER 48

Non-Reflective Multi-Directional Wave Generation by Source Method

Masahiro Tanaka[1], Takumi Ohyama[1], Tetsushi Kiyokawa[1],
and Kazuo Nadaoka[2]

Abstract

A new wave-generation system, composed of a source and an absorber, is proposed to realize a non-reflective wave field in a laboratory basin as an advanced alternative to conventional methods. Theoretical studies based on the linear potential theory were carried out to investigate the characteristics of wave fields generated by the proposed method. Performance of the new system was compared to that of conventional *serpent-type* wave-makers. The proposed system was founded to provide a significantly larger effective area for multi-directional waves than does the serpent-type wave makers.

Experimental studies using a two-dimensional wave tank were also conducted to verify the performance and practicality of the new system. The results showed that the new devised equipment can produce a nearly non-reflective wave field and can generate waves efficiently even in deep water.

1. Introduction

Serpent-type wave-maker has been developed to generate multi-directional irregular waves, and has been introduced in many laboratories (Biesel, 1954; Gillbert, 1976; Takayama, 1982). However, this wave-generation system has not yet solved two serious problems. First, re-reflected waves from wave-generating paddles and side walls of a tank disturb the wave field around a model after certain time passed.

1 Institute of Technology, Shimizu Co., 3-4-17, Etchujima, Koto-ku, Tokyo 135, Japan
2 Tokyo Institute of Technology University, 2-12-1, Ohokayama, Meguro-ku, Tokyo 152, Japan

The second problem is that the effective wave area decreases according to increase of the incidence angle of waves.

Funk·Miles (1987), Isaacson (1989) and Dalrymple (1989) have proposed a directional wave-making method considering side-wall reflection to expand an effective wave field.   Although this method can slightly widen the effective wave field by controlling reflection waves at side wall, proportion of ineffective wave area in the tank is still large.

On the other hand, Hirakuchi et al. (1991) and Ikeya et al. (1992) have proposed an active directional wave absorption method.   In this method, the reflection waves are absorbed by controlling the amplitudes and phases of each paddle corresponding to the heights, phases and directions of the reflection waves.   Since this method requires measurement and analysis of a significant amount of waves to control the wave-generating system in an instant time, it is quite difficult to apply to an actual system.

We have devised a non-reflective multi-directional wave-generating system that consists of a distributed wave making source and a wave absorber without using wave-generating paddles.

2. Concept of the New System

The wave-generation system consists of a circular wave-making source and an external wave absorber arranged in a circular tank as shown in Fig. 1.   The idea of the proposed method is founded on the principle of two-dimensional numerical wave-generating model (Brorsen·Larsen, 1987; Ohyama et al., 1991).   The two-dimensional numerical model employs an effective non-reflective open boundary treatment so that it can be applied to arbitrary wave fields including nonlinear random waves.

The proposed system generates waves by pumping water in and out without using paddles, and the heights and direction of waves are controlled by the intensity and phase of the source.   Since this source method does not involve wave paddles unlike conventional wave-makers, it is expected that the reflected waves from model objects permeate through the source without re-reflection, and are absorbed by the external absorber.   In addition, since the wave-making source is arranged in a circular shape, an effective wave field is independent of wave directions, whereas the performance of the conventional *serpent-type* wave-makers is significantly direction-dependent.

For practical application, the wave-making source can be composed of a series of

small units mounted in a concentric semicircle. It would require careful provision to minimize the reflection from the source. A practical equipment and its performance of wave generation are shown in Section 4.
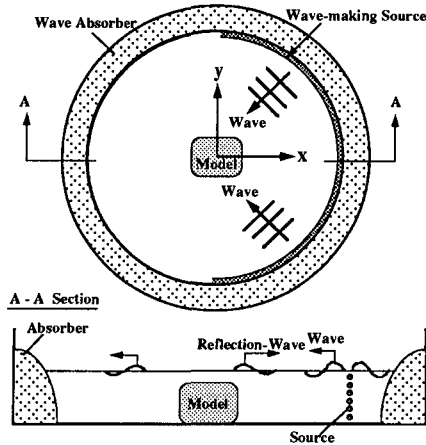
Fig. 1   Concept of non-reflective multi-directional wave generation by source method

3. Theoretical Analysis

3.1 Theoretical Formulation

Multi-directional irregular waves are composed of waves with various periods, heights and directions. Since the performance of waves generated by the source method is independent of wave direction, it can be evaluated by using single-directional regular waves.

The coordinate system and definition sketch used in this study are shown in Fig. 2. With the assumption of incompressible, inviscid fluid, and irrotational flow, the fluid motion can be described with a velocity potential, ϕ $(r, \theta, z)e^{-i\omega t}$. The potential satisfies the following Poisson's equation within the fluid domain and which is subject to boundary conditions at the free surface and the tank bottom.
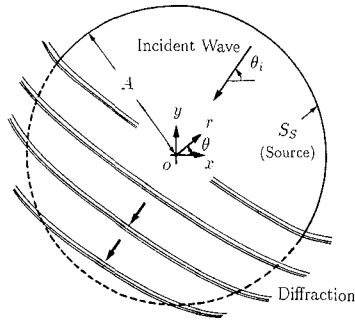
$$\nabla^2 \phi = U^*(\theta, z)\delta(r - A) \tag{1}$$

Fig. 2   Definition sketch of theoretical model

Where, U^* is the source intensity of formulated by Brorsen et al. (1987), δ: Dirac's Delta function, and A: distance (radius) between the center of a tank and a wave making source.   Applying the Green's function method to Eq. 1, the velocity potential, $\phi(P)$, at an arbitrary point in a basin, P (r_p, θ_p, z_p), is expressed as

$$\phi(P) = -\frac{1}{4}\int_{S_s} U^* G \, ds \qquad (2)$$

in which, S_S denotes the surface of wave-making source, and G: the Green's function derived by John (1950) as shown in Eq. 3 and 4.

$$G = \frac{2\pi i (\kappa^2 - v^2)}{h(\kappa^2 - v^2) + v} \cosh k(h + z_p)$$
$$\cdot \cosh k(h + z) H_0^{(1)}(\kappa R_P) + \sum_{n=1}^{\infty} \frac{4(\kappa_n^2 + v^2)}{h(\kappa_n^2 + v^2) - v}$$
$$\cdot \cos \kappa_n(h + z_P) \cos \kappa_n(h + z) K_0(\kappa_n R_P) \qquad (3)$$

$$R_P = \sqrt{(r_p \cos \theta_p - r \cos \theta)^2 + (r_p \sin \theta_p - r \sin \theta)^2} \qquad (4)$$

Where, k: wave number, k_n: eigenvalue, $H_0^{(1)}$: Hankel function, K_0: Bessel function, $v = \omega^2/g$, g: gravity acceleration.

    Since waves generated by a source progress to both sides of the source, the intensity of the source can be given as the following equation (Brorsen·Larsen, 1987).

$$U^*(\theta,z) = 2\frac{\partial \phi_i}{\partial r}\bigg|_{r=A} \qquad (\theta_i - \frac{\pi}{2} \le \theta \le \theta_i + \frac{\pi}{2}) \qquad (5)$$

Substituting the potential ϕ_i to Eq. 5, the intensity U^* can be expressed as shown in Eq. 6.

$$U^*(\theta,z) = -ik\cos(\theta - \theta_i)\frac{gH_i}{\omega}\frac{\cosh k(h+z)}{\cosh kh}e^{-ikA\cos(\theta-\theta_i)}$$

$$(\theta_i - \frac{\pi}{2} \le \theta \le \theta_i + \frac{\pi}{2}) \qquad (6)$$

Substituting Eq. 3 and 6 into Eq. 2, analytical form of the potential $\phi(P)$ at an arbitrary point P in a tank can be obtained as follows:

$$\phi(P) = \frac{gH_i}{2\omega}\varphi(r_P, \theta_P)\frac{\cosh k(h+z_P)}{\cosh kh} \qquad (7)$$

$$\varphi = -\frac{kA}{2}\int_{\theta_i - \frac{\pi}{2}}^{\theta_i + \frac{\pi}{2}}\cos(\theta - \theta_i)\, e^{-ikA\cos(\theta-\theta_i)}H_0^{(1)}(k\hat{R}_p)\,d\theta \qquad (8)$$

$$\hat{R}_p = \sqrt{(r_p\cos\theta_p - A\cos\theta)^2 + (r_p\sin\theta_p - A\sin\theta)^2} \qquad (9)$$

3.2 Definition of Performance of Wave-generation

Performance of a wave generating system is generally evaluated with areal extent of effective wave-field.   The effective area is defined as an area, in which errors of wave heights and directions from an intended wave are smaller than allowable tolerances, as shown in Fig. 3.   The wave height and direction errors, ΔH and $\Delta\theta_w$, are described as shown in Eq. 10 and 11.

$$|\Delta H| / H_i = |H - H_i| / H_i \qquad (10)$$

$$|\Delta\theta_w| = |\theta_w - \theta_i| \qquad (11)$$

By defining the extent of the effective wave-field as a ratio of the effective zone's radius to that of basin, a/A, its dependence on incident wave-direction can be eliminated.
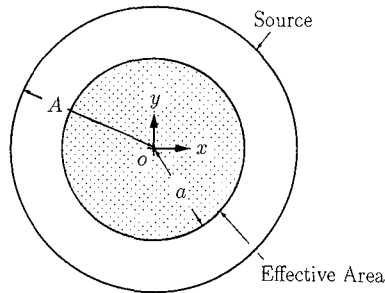
Fig. 3   Definition of effective wave area

3.3 Performance of wave-generation by the source method

Characteristics of wave field generated by the source method were examined using a theoretical model (see Fig. 1).   In this calculation, non-reflection waves from the wave-making source and the absorber behind the source were assumed.

Wave-heights distributions normalized with an incident wave height is shown in Fig. 4 (a).   Where, a tank radius is 3 times of the wave-length ($A/L = 3.0$).   Fig. 4 (b) and (c) describe vectors of energy flux and distributions of wave-direction errors at $A/L = 3.0$, respectively.   It can be seen in Fig. 4 (a) that the relative wave-height errors, $|(H - H_i)|/H_i$, are less than 0.05 in the wide area of the tank.   The wave-direction errors are less than 5 degrees in the almost all the area as shown in Fig.4 (c). These results indicate that the proposed source method can provide the effective wave field in the wide area of the tank.

Distributions of normalized wave-height and wave-direction errors at $A/L = 1.0$ are shown in Fig. 5 (a) and (b), respectively.   The magnitudes of both errors for this case are much bigger than those for the case of $A/L = 3.0$.   This difference indicates that A/L is a significant parameter in the design of the proposed system.

Fig. 6 (a) shows the dependence of the a/A on the parameter A/L, when the error tolerance $(|\Delta H|/H_i)_{max}$ is varied from 0.05 to 0.2 with $|\Delta\theta_w|_{max}$ fixed at 4 degrees. Fig. 6 (b) also shows characteristic of a/A versus A/L corresponding to variation of wave-direction error, $|\Delta\theta_w|_{max}$, when $(|\Delta H|/H_i)_{max}$ is fixed at 0.1.   It is seen that the effective area generally increases with A/L.   The effective wave area can be evaluated using the results shown in Fig. 6 (a) and (b).   For example, assuming allowable tolerance to be $(|\Delta H|/H_l)_{max} = 0.1$ and $\Delta\theta_w = 4$ degrees, when the tank radius is set at 2.4 times of incident wave-length, an area of about 80% radius in the tank is provided as the effective wave field.
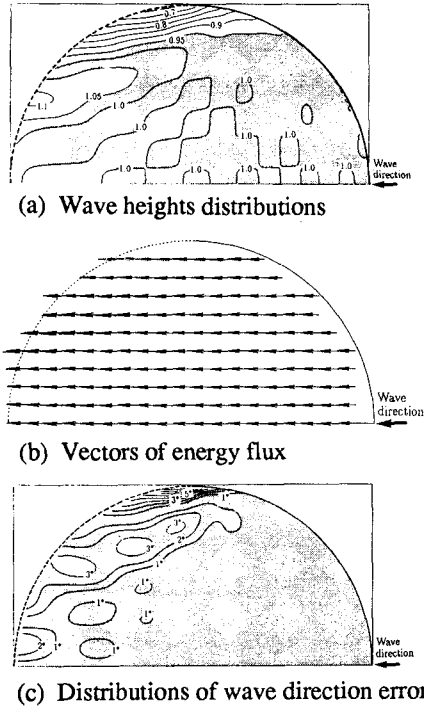
(a) Wave heights distributions

(b) Vectors of energy flux

(c) Distributions of wave direction error $\Delta\theta_w$

Fig. 4   Wave field generated by the source method $(A/L = 3.0)$

(a) Wave heights distributions

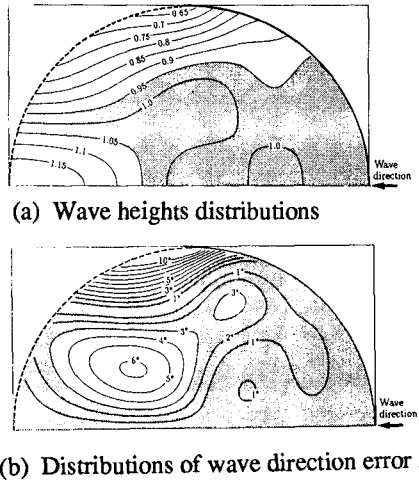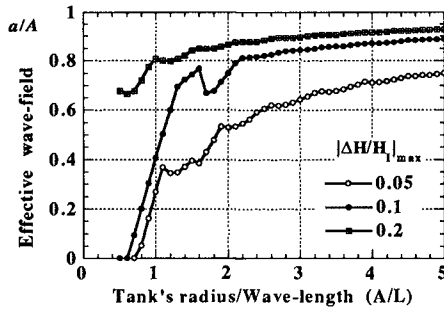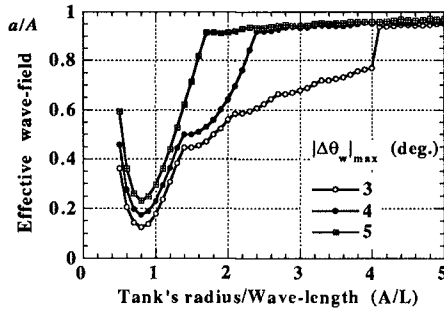(b) Distributions of wave direction error $\Delta\theta_w$

Fig. 5   Wave field generated by the source method $(A/L = 1.0)$

(a) Effective wave field with $|\Delta H/H_1|_{max}$

(b) Effective wave field with $|\Delta\theta_w|_{max}$

Fig. 6 Effective wave field by the source method

3.4 Comparison with serpent-type generator

Wave fields generated by a serpent-type wave-maker was simulated using a theoretical model (Dalrymple, 1989) to compare with performance of the proposed source method. In this calculation, the serpent-type generator was controlled so as to widen the effective wave field by using the side-wall-reflection of the tank.

Fig. 7 (a) and (b) show computed results of water-elevation distribution and vectors of energy flux of waves generated by a serpent-type. Where, the ratio of the tank width to wave length, B/L, and the incidence angle of wave, θ_i, are fixed at 6.0 and 40 degrees, respectively. In this case, the serpent-type wave generator was controlled so as to provide the best performance at x=0.

Although the serpent-type generator produces uniform wave field in the central area of the tank, it causes standing wave and diffraction waves at the corners and their
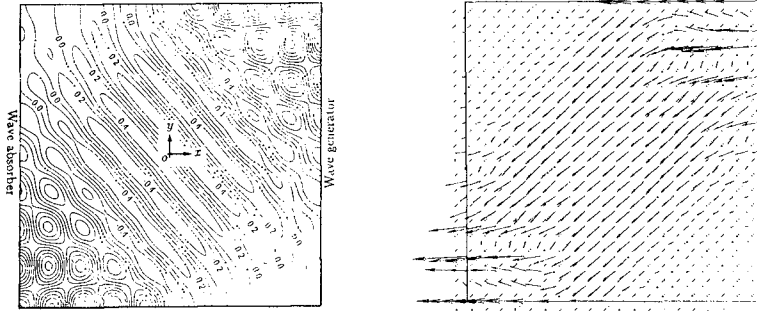
(a) Water elevation distributions   (b) Vectors of energy flux

Fig. 7   Wave field generated by a serpent-type $(B/L = 6.0)$
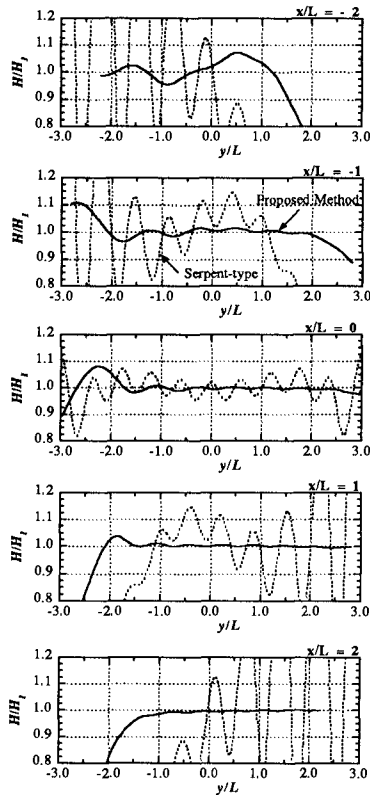

Fig. 8   Comparison of wave height distributions between
for the source method and a serpent-type

perimeters. It can be seen in these areas that the magnitudes and directions of energy flux are different from those of the intended waves. As the results, the serpent-type generator provides large ineffective wave field in the tank. The effective wave-field of the serpent-type depends on incident wave directions, decreasing with increase of the incidence angle of waves.

In Fig. 8, normarized wave-height distributions at cross-sections of x/L = -2, -1, 0, 1 and 2 generated by a *serpent-type* are compared with those generated by the source method using the results shown in Fig. 4 (a) and 7 (a). The results show that the source method generates waves much more uniformly than does the *serpent-type* not only at x/L = 0.0, where the serpent-type gives the best performance, but also at x/L = ±1.0 and ±2.0. It is expected, therefore, that the proposed source method can provide significantly larger effective fields for multi-directional waves compared to those provided by *serpent-type* wave makers.

4. Application of the source method

4.1 A devised equipment

We have carried out preliminary examinations of various devices to evaluate practicability of a wave-making source. As a result, a device, which supplies and discharges water at tank bottom, has proved to be the most practical source. The principle behind wave-generation by this device is similar to that by a non-reflective wave-making system devised by Goda (1965): it generates a vertically oscillating flow at channel bottom by using a paddle as shown in Fig. 9. The Goda's method was not of practical use because of inefficiency for deep water wave-generating. In addition, the method requires elaborate work to keep nearly water-tightness in an interstice between the pit's walls and the wave paddle.
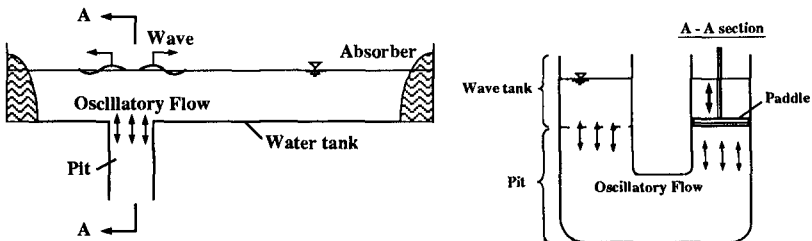

Fig. 9   Non-reflective wave generator with vertical oscillatory flow

To solve these problems, authors have made over this method into a practical equipment, which consists of pumps, valves, and an adjustable pit, as shown in Fig. 10. Vertical oscillating flow by using the pumps, valves and adjustable pit instead of using a wave-paddle: the pump P_I supplies water into the pit, and the pump P_O discharges water from the pit. Wave heights and periods are controlled by using two valves, V_I and V_O. The pit's height and width, d and B, can be adjusted to improve the efficiency of wave generation in deep water (see Fig. 10).
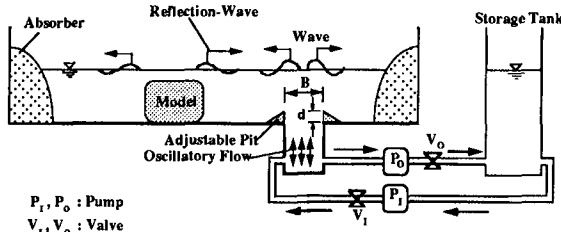

Fig. 10 A practical equipment of the source method

4.2 Performance of wave-generation by the equipment

It is important for the equipment to produce wave field with negligible reflection from the pit and to improve efficiency of wave generation in deep water. To evaluate the effects of the pit's width and height on characteristics of the reflection waves and the efficiency, experiments were carried out using a two-dimensional wave tank. The coefficient of reflection waves caused by the pit is calculated using Eq. 12 (Goda et al., 1964).

$$K_R = \frac{H_{max} - H_{min}}{H_{max} + H_{min}} \qquad (12)$$

Where, H_{max} and H_{min} are heights of standing wave in front of a vertical wall apart from the pit by N and $(N+1/2)$ times of a half wave length, respectively (N: an integer). On the other hand, the wave generation efficiency is evaluated using a ratio of a wave height to oscillatory flow amplitude in the pit. Calculations were also conducted to estimate the performance of the wave-generating pit by Green function method. As theoretical formulation about the wave generation pit has been described by Tanaka et al. (1993), only a definition sketch of the theoretical model is shown in Fig. 11.
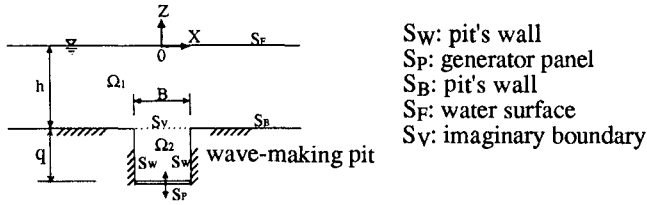
S_W: pit's wall
S_P: generator panel
S_B: pit's wall
S_F: water surface
S_V: imaginary boundary

Fig. 11 Definition sketch of a theoretical model of
the wave making pit

Fig. 12 (a) shows response of reflection coefficients, K_R, to parameter, h/L, as B/h was varied from 1.2 to 3.2.   In this case, the top of the pit is set at the same level of the tank bottom.   Fig. 12 (b) also shows the dependence of wave generation efficiency, $H/2e$, on h/L upon the same conditions with Fig. 12 (a).   Where, h is the water depth of the tank, L: the wave length, B: the width of the wave-making pit, and $2e$: an amplitude of the oscillatory flow in the pit.   In the figures, solid lines denote the computed results.   Although the experimental and the numerical results agree on the characteristics of $H/2e$, both results show large discrepancies in the characteristics of K_R.   Since the detailed reason for the discrepancies has not been made clear, the characteristics of K_R for the new equipment are evaluated using the experimental results in this paper.

Although the increase in B/h improves the wave-generating efficiency of the equipment, it enlarges the reflection waves from the pit.   Therefore, B/h should be set so that the equipment can achieve low reflection wave over a wide range of wave periods: K_R is 0.15 or less for B/h = 1.5, and further decreases to around 0.1 for B/h =1.2.

In Fig. 13 (a), the effect of the pit height on the efficiency of wave generation is shown when d/h was varied 0, 0.305 and 0.432.   Where, B/h' = 1.2, B = 30 cm, d: the pit height, h': depth between water surface and the top of the pit ($h = d + h'$).   The wave-generation efficiency with d/h = 0.305, 0.432 is significantly improved in the range of $h/L > 0.3$ compared with that with d/h = 0. These results indicate that the adjustment of the pit height is effective for the improvement of the wave generation efficiency.   In addition, the former maximum efficiencies are greater than the latter one.

Fig. 13 (b) shows characteristics of the reflection waves caused by the pit.   The experimental conditions are the same with those of Fig. 13 (a).   This equipment can achieve low reflection over a wide range of wave periods even when d/h is set at
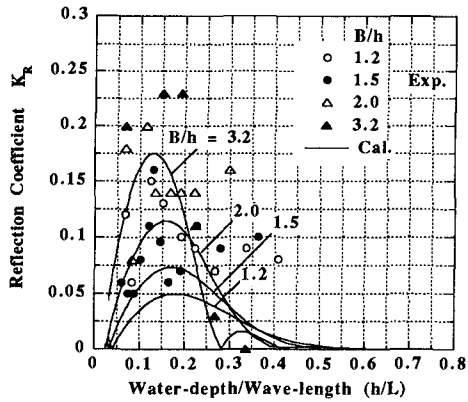
(a) Coefficients of reflection waves from the pit
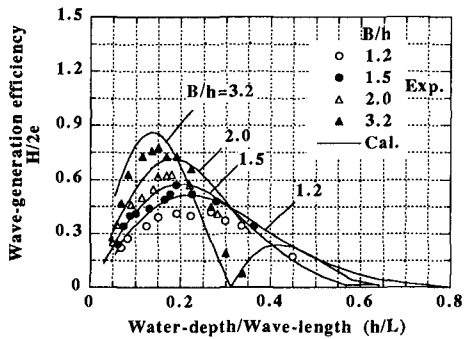
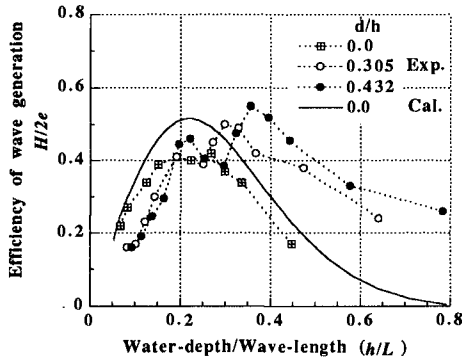

(b) Efficiency of wave generation

Fig. 12 The effects of pit width, B, on performance of wave generation
($d/h = 0.0$)

0.305 or 0.432. The results of Fig. 13 shows that the adjustable pit can improve the efficiency of the wave generation without increasing reflection waves.

From the experimental results, the proposed equipment can generate wave with negligible re-reflection from the wave-generating pit, and can efficiently make deep water waves.

It is expected that the equipment would provide nearly non-reflective wave field for multi-directional wave-generation by arranging a series of the units in a concentric semicircle in circle tank.

(a) Efficiency of wave generation
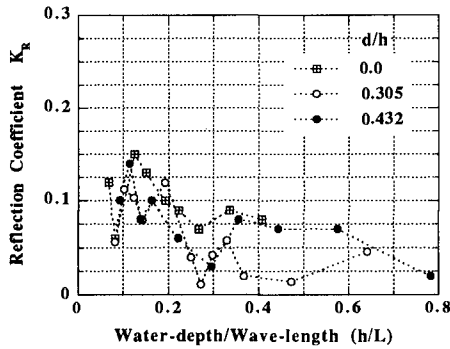
(b) Coefficients of reflection waves from the pit

Fig. 13 The effects of pit height, d, on performance of wave generation
($B/h' = 1.2$)

5. Conclusions

Wave-generation by source method, which does not depend on wave-making paddles, has been proposed to produce non-reflective multi-directional waves in a laboratory basin.   The characteristics of wave fields generated by the source method were evaluated using a theoretical model.   A practical equipment with a wave-making pit at channel bottom was devised to realize the source method, and the performance of the wave-generation was also examined.   Major findings of the present study are summarized as follows:

1) The wave generation by the source method provides significantly larger effective area for multi-directional waves than does the *serpent-type* wave makers.

2) The equipment with a wave-making pit at a channel bottom can produce wave field with negligible reflection by adjusting the width and position of the pit, and can also efficiently generate waves in deep water.

References

Biesel, F. (1954):   Wave machines, Proc. 1st Conf. on Ships and Waves, pp.121-125.

Brorsen, M. and J. Larsen (1987): Source generation of nonlinear gravity waves with the boundary integral equation method, Coastal Eng., Vol. 11, pp. 93 - 113.

Dalrymple, R. A. (1989):   Directional wavemaker theory with side wall reflection, Jour. Hydraulic Research, Vol. 27, No. 1, pp 23-34.

Funke, E. R. and M. D. Miles (1987):   Multi-directional wave generation with corner reflectors, National Research Council Canada, Hydraulic Laboratory, Tech. Rept., No. TR-HY-021.

Gilbert, G. (1976):   Generation oblique waves, Hydraulics Research Station, Wallingford, England, Notes 18, pp. 3-4.

Goda, Y. and T. Kikura (1964):   The generation of water waves with a vertically oscillating flow at a channel bottom, Report of Port and Harbor Tech. Res. Inst., No.9, pp. 1-24.

Hirakuchi, H., Y. Kajima, H. Tanaka and T. Ishii (1991):   Characteristics of absorbing directional wavemaker, Proc. 38th Japanese Conf. on Coastal Eng., pp. 121-125 (in Japanese).

Ikeya, T., Y. Akiyama and K. Imai (1992):   Active Directional Wave Absorption Theory, Proc. 39th Japanese Conf. on Coastal Eng., pp. 81-85 (in Japanese).

Isaacson, M. (1989):   Prediction of directional waves due to a segmented wave generator, Proc. of 23rd Congress of the Int. Asso. Hydraulic Res. Vol. C, pp. 435-442.

John, F. (1950):   On the motion of floating bodies II, Comm. Pure and Appl. Math., Vol. 3, pp. 45 - 101.

Ohyama, T. and K. Nadaoka (1991):   Development of "Numerical Wave Tank" in nonlinear and irregular wave field with non-reflecting boundaries, Jour. of Hydraulic, Coastal and Environmental Eng., JSCE, Vol.429 II-15, pp. 77-86.

Takayama, T. (1982):   Theoretical properties of oblique waves generated by serpent-type wave-maker, Report of Port and Harbour Research Inst., Vol. 21, No.2, pp. 3-48.

Tanaka, M., T. Ohyama and T. Kiyokawa (1993):   Performance of non-reflective wave generator, Proc. 40th Japanese Conf. on Coastal Eng., pp. 41-45 (in Japanese).

The Growth of Wind Waves in Shallow Water

L.A. Verhagen and I.R. Young
Dep. of. Civil Engineering, University College, University of New South Wales,
Canberra, Australia

Abstract
The field experiment at Lake George has brought valuable data that was not yet available. The analyses done to the data has shown new insights into shallow water waves. Already from the first analyses we can derive some interesting things. The one-dimensional shallow water spectra seem to have a clear peak enhancement and tail that is proportional to $f^{-4.5}$. The directional spread with two-dimensional spectra shows at the higher frequencies (twice the peak frequency) the waves move symmetrically at an angle with the wind. More analysis needs to be done to fit different kind of spectra and to find a function for the directional spread.

Introduction
Although most coastal engineering activity is in regions of shallow water, there is little know about the growth of shallow water waves. Many numerical models attempt to incorporate the growth with relationships which are mostly derived from deep water data. The lack of reliable field data in shallow water is a major problem. To overcome this lack of data, a large field experiment is being conducted to study the growth of shallow water waves. The experiment has been set in Lake George (25 km x 12 km) (fig 1) just north of Canberra (Australia). The lake has a flat bed with an approximate depth of 2 meters. There are no high obstacles around the lake to influence the wind significantly.

Experiment
Eight wave measuring stations have been established along the north-south axis of the lake (fig 1). Data from these stations are sent by telemetry to a station on the shore where they are logged. The data, after analysis, yield one-dimensional spectra. At station 6, located in the centre of the lake, there is also a cluster of 7 wave measuring gauges to determine the
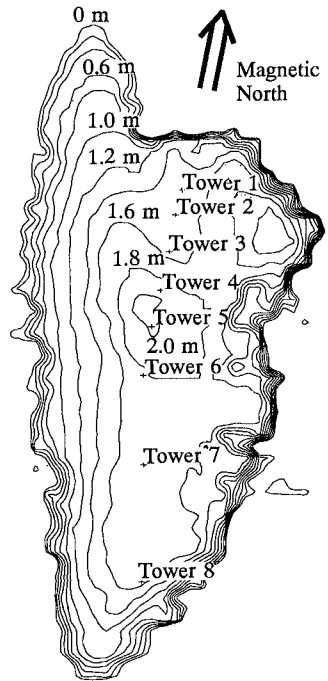

Figure 1
The bathometry of lake George and the position of the wave measuring towers. Note the platform is at tower 6.

665

directional spread. The wind speed and direction are measured at 5 locations along
the lake. At various sites other meteorological data such as air and water
temperature, air humidity, and solar radiation are also measured.

Seven wave measuring
stations are nearly identical.
They are space-frame towers,
with a wave measuring
device mounted on the
side (fig 2). The towers are
moored to the lake bed by 4
guy wires which were
anchored into the bed. The
wave measuring devices are
Zwarts poles (Zwarts 1974).
The Zwarts poles consist of
an aluminium outer (55 mm)
and inner pole (20 mm)
which determine the
electrical properties. These
wave measuring devices
have the advantage that the

Figure 2
Details of the tower. From left to right; the aerial to send back the
data by telemetry. The box with batteries the radio and the
electronics box for the ZWARTS pole, just in front the
anemometer mast and the hydrometer, on top the solar cell, and
on the back side the ZWARTS pole.

they do not require much maintenance. Other wave measuring devices like

resistance gauges, capacitance
gauges or waverider buoys needed
too high level of maintenance or
are outside the frequency range of
the waves on Lake George. The
poles were calibrated both
dynamically and statically in the
lab. The data were send to a base
station on the shore via a telemetry
link. The radio was powered by
two solar cells on the top of the
tower (fig 2). At five of the towers,
there were 10 meter high masts
with an anemometer on top (fig 3).

Figure 3
A complete view of one of the towers with a 10
meter anemometer mast.

At two towers the air humidity and temperature (fig 2) were measured together with
the water temperature at three levels (0.5, 1 , 1.5 meters for the lake bed).

Wind Analysis
The wind was measured at 5 stations (stations 2,4,6,7,8) on the lake. However there
was only a very short time period that all 5 anemometers were working. The
anemometer on the platform (station 6) worked most of the time. All anemometers

were mounted on 10 meter high mast above the water surface. The anemometer on the platform (station 6) was a "Young" anemometer and the anemometers on the towers were "VDO" anemometers.

A major problem is knowing the exact wind speed along the fetch. This is a serious problem when there is a change of roughness length of the surface (e.g. from land to water). Taylor (1984) gives some guidelines. The basic principle is that the boundary layer adjusts it self after a certain length. The flow will have an internal boundary layer with a depth of δ_i. Outside this internal boundary layer the wind velocity is the as equation 1.

$$U_z = \frac{U_*}{\kappa} \ln\left(\frac{z}{z_o}\right)$$
(1)

In which Z is the elevation at which U_z is measured. κ is the von Karman's constant ($\kappa = 0.4$), Z_o is the roughness length of the surface and U_* is the friction velocity. The internal boundary layer grows according to

$$\delta_i = 0.75 \, Z_0 \left(\frac{x}{Z_0}\right)^{0.8}$$
(2)

Where x is the distance along the fetch and Z_0 is the roughness length at x. Inside the boundary δ_i layer the wind speed at elevation Z is

$$U_z = \frac{\ln\left(\frac{Z}{Z_0}\right) \ln\left(\frac{\delta_i}{Z_{0u}}\right)}{\ln\left(\frac{\delta_i}{Z_0}\right) \ln\left(\frac{Z}{Z_{0u}}\right)} \, U_{0u}$$
(3)

With Z_{0u} being the roughness length of the upwind boundary, U_{0u} the upwind wind velocity and U_z the wind speed at elevation Z. The wind is usually only measured at a point or a few points along the fetch. As indicated in equations 2 & 3 the wind speed varies after a change of roughness length. Since the wave growth is dependent on the wind speed it is wise to calculate an average wind speed for the fetch. One could also argue that even a mean of the wind speed along the fetch is not good enough and a more sophisticated average should be taken.

We tested the Taylors (1984) method with the data set when all five anemometers were working. The results from the theory and the measured wind speeds were nearly the same. Therefore the anemometer at station 6 (the platform) was used to calculated the wind speed along the north south fetch for each event.

There is a large debate about which wind speed to use, in the making the wave height, wave frequency, fetch and water depth dimensionless. In general the wind speed is measured at 10 meters above the surface level. If the wind speed is measured at a different level it can be converted to U_{10} using the logarithmic form of the boundary layer (see equation 1). There are several other wind speeds to make the wave height, wave frequency, fetch and water depth dimensionless. They are usually based on either the friction velocity like Wu (1980) describes, the inverse wave age (U/c_p) like Donelan (1985) argues, or a combination of both like HEXOS (Smith et al. 1992). The wind speed used here was the wind speed measured at 10 meters above the surface, because the other did not give a clear advantage and they were not measured directly.

Growth Curves

The fetch limited growth curves for shallow water have two limits. One limit is the JONSWAP (Hasselmann et al. 1973) deep water growth, and the other is the maximum wave height by a finite depth and wind speed. Vincent in his first paper (1985) suggested that the relation between dimensionless water depth and dimensionless wave height,

$$\frac{H_s g}{u^2} = \left(\frac{d g}{u^2} \right)^{0.5} \qquad (4)$$

Where H_s is the significant waveheight, d the waterdepth, g the gravitational constant and u the wind speed at 10

Figure 4
Lake George Data. Dimensionless waterdepth is set out against dimensionless waveheigth. Note the spreading in the wave data with wind speeds greater than 3 m/s is caused by the fact that not all the wave are fully developed.

meters above the surface. Later Vincent and Hughes (1985) had taken measurements from Lake Okeechobee (Florida, USA) to determine the maximum dimensionless wave height. From these data and from an analytic procedure, they suggested that the relation between dimensionless water depth and dimensionless wave height was
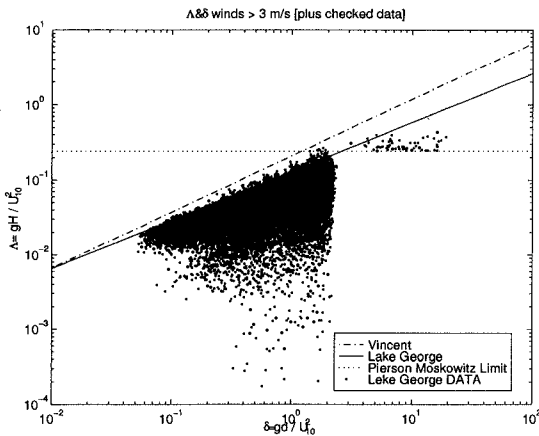
$$\frac{H_s g}{u^2} = \left(\frac{d g}{u^2}\right)^{0.75} \tag{5}$$

Data from Lake George was used to test this. All the data from Lake George with wind speeds greater than 3 m/s were used together with selected data where the wind speed was smaller than 3 m/s. These last data were selected if the wind speed and direction were constant 8 hours before and 3 hours after the event. The Lake George data tend to indicate a less steep slope than what Vincent and Hughes suggested (fig 4). If one projects the Lake Okeechobee data on a graph similar to the Lake George data (fig 5) one can see that the Lake Okeechobee has the same tendency. Purely on empirical grounds the following seems to be more appropriate.

$$\frac{H_s g}{u^2} = \left(\frac{d g}{u^2}\right)^{0.65} \tag{6}$$

The upper limit for the growth in deep water is the Pierson Moskowitz limit (1964). Pierson Moskowitz (1964) proposed, integrating the spectrum resulting in a limit

$$\frac{H_s g}{u^2} = 0.2433 \tag{7}$$

Vincent and Hughes (1985) do not have a limit because they had not found evidence for this. Data for this limit is indeed very hard to find because of the long fetch and time necessary for the full development of the waves. This only happens during very low wind speeds. Because of swell and other wind waves generated elsewhere it is very hard to measure the growth of smaller waves in ocean environments. However in a lake this possible. During the Lake George experiment there were a number of these events. These events were specially selected because of the tendency of the wind varying in both speed and direction at low wind speeds. The events selected with wind speeds lower than 3 m/s had to a have a constant wind speed and wind direction, during a period of 8 hours before and 3 hours after. In figure 4 the Pierson Moskowitz limit with the selected data is shown.

It is believed that the lake sides have a small influence on the observed growth rates. Attempts to measure this effect using three different numerical models have been unsuccessful. The models [WAM (WAMDI 1988), HISWA (Holthuijsen et al.1988), ADFA1 (Young 1988)] produced conflicting results and all significantly deviate from the observed data. Therefore no correction factors have been applied to the data to compensate for the sides of the lake.

In general the data are
consistent with the
commonly used CERC
(SPM 1984) growth
curves, but at small
values of dimensionless
fetch tend to yield lower
dimensionless energy.
This could be due to the
effects of the change in
surface roughness length
between land and water.
Because of this and
because of uncertainty in
determining the exact
location of the upwind
boundary, the fetch of the
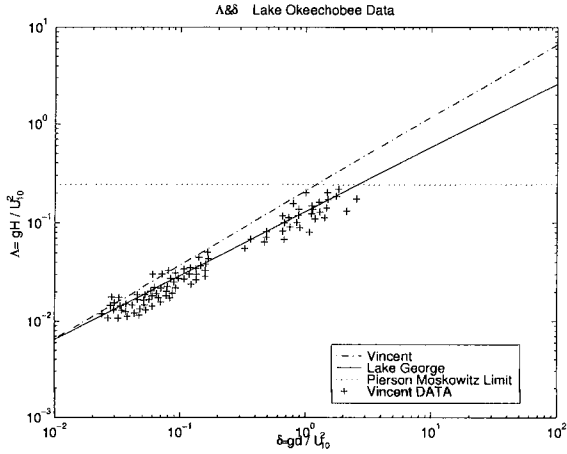first station is set equal to
the corresponding
JONSWAP (Hasselmann
et al. 1973) result for the
observed energy. From the data new curves were calculated (fig 6 and fig 6).

Figure 5
The same graph as with the Lake George data, except with the
Lake Okeechobee data. The Lake George line looks like a better
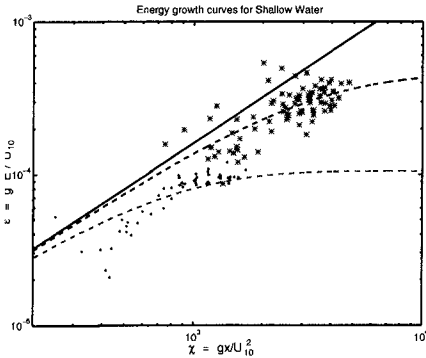estimate.

Figure 6
Two growth curves for dimensionless Energy set
out against dimensionless fetch. The curves are
calculated from the points with the same
dimensionless depth. The most upwind point is
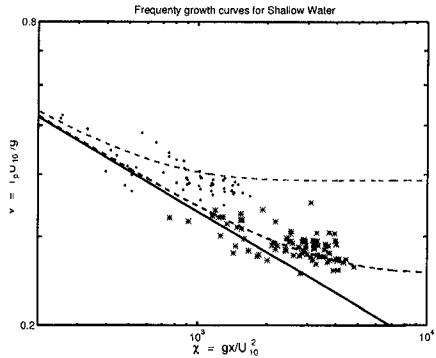set on the deep water growth (JONSWAP,
Hasselmann et al. 1973)

Figure 7
Two growth curves for dimensionless frequency
set out against dimensionless fetch. The curves
are calculated from the points with the same
dimensionless depth. The most upwind point is
set on the deep water growth (JONSWAP,
Hasselmann et al. 1973)

One-Dimensional Spectra

The one-dimensional spectrum has some of the characteristics of deep water spectra. The data used in the analyses of the spectra along the lake is only during north and south wind events with wind speeds greater than 3 m/s. In figure 8 the spectral peak moves toward lower frequencies as the fetch increases. In figure 8 one can see a small but very distinct peak enhancement. The spectra decay with $f^{-4.5}$ from the peak frequency (f_p) until approximately 3 f_p, and at f^{-5} at higher frequencies (fig 9). The decay of f^{-5} however could be caused by a doppler shifting of the high frequency waves "riding" on the back off lower frequency waves. More analyses of these one-dimensional spectra are under way, including the differential growth between the wave measuring stations.
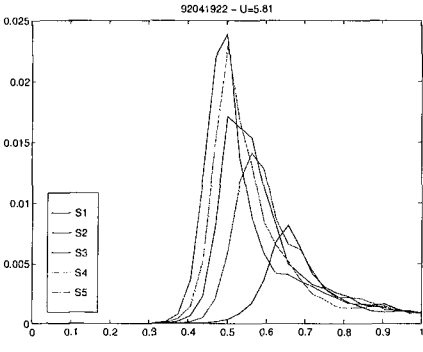

Figure 8
Different stages of the spectra during growth. The spectral peak moves toward the lower frequencies as the fetch (or growth) increases. The peak enhancement can easily be seen. The frequency is set out against the Energy
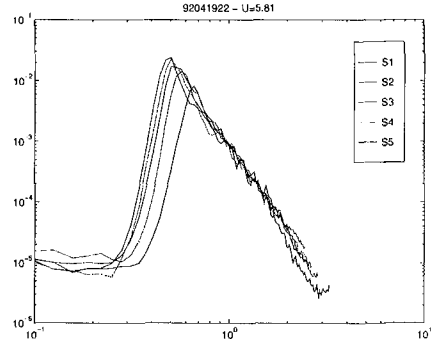
Figure 9
This is a loglog plot of the different stages of the spectral growth. The Energy decays in the tail of the spectrum is related to $f^{-4.5}$. At higher frequencies the Energy decay is related to f^{-5}. The frequency is set out against the Energy

Two-Dimensional Spectra

At the platform (station 6) the directional spectra were measured by an array of 7 Zwarts poles. The array could be operated by modem via the base station from the University College. The array was formed like a Mercedes star (Young 1995). For the analyses the Maximum Likelihood Method (MLM) was used. This method has the advantage over the Maximum Entropy Method (MEM) that it does not produce false peaks. The disadvantage is that the MLM produces a broader spectrum and has trouble analysing bi-modal seas. Lake George however, does not have any bi-model seas.

Due to the large number of wave measuring gauges in the array, the directional resolution is much higher than pitch-roll buoys or p, u, v meters. In figure 10 the normalised directional spreading function at $\frac{1}{2}f_p$, f_p, $2f_p$ and $3f_p$ is shown. The spectrum at f_p is quite narrow and aligned with the wind direction. However at $2f_p$

and $3f_p$ the spectrum is quite broad and develops a bidirectional mode, with more energy propagating at an angle to the wind than in the wind direction.

Conclusions

The first analyses look promising. However more work needs to be done in analysing all the data. We are trying to fit different types of spectra like the JONSWAP and TMA spectra to see which fit better and with which parameters. With the Two-Dimensional Spectra we are trying to fit a spreading function that is dimensionless frequency depended.
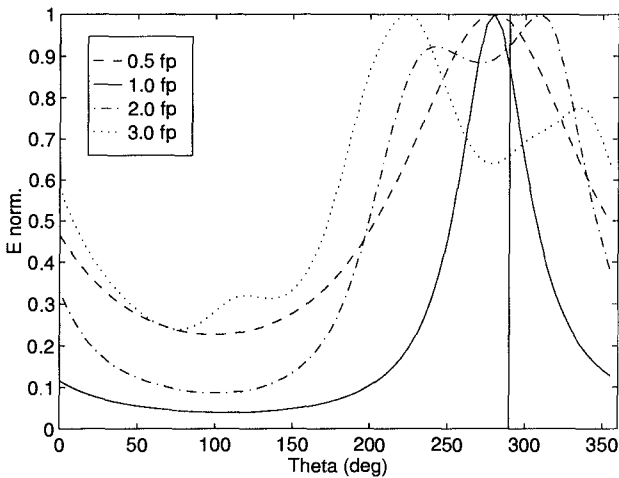
Figure 10
Cuts of the directional spectra at $\frac{1}{2}f_p$, f_p, $2f_p$ and $3f_p$. The spectrum has one peak at frequency smaller than $2f_p$. The waves are travelling in the direction of the wind (thick line). However at frequencies greater than $2f_p$ there is splitting of the directional spread. This means that the waves are travelling at an angel with the wind.

References

Donelan M.A., Hamilton J. and Hui W.H. 1985. Directional Spectra of Wind-Generated Waves. Phi. Trans. R. Soc. Lond. A 315, pp. 509-563

Hasselmann K., Barnett T.P., Bouws E., Carlson H., Cartwright D.E., Enke K., Ewing J.A., Gienapp H., Hasselmann D.E., Kruseman P., Meerburg A., Müller P., Olbers D.J., Richter K., Sell W., Walden H. 1973. Measurements of Wind-Wave Growth and Swell Decay during the Joint North Sea Wave Project (JONSWAP), Deutsches Hydrographisches Institut, Hamburg

Holthuijsen L.H., Booij N. and Hebers T.H.C. 1988 "A prediction model for stationary short-crested waves in shallow water with ambient currents", Coastal Engineering, 13, 23-54

Pierson W.J. and Moskowitz L. 1964. A proposed Spectral Form for Fully Developed Windseas Based on Similarity Theory of S.A. Kitaigorodskii, Journal of Geophysical Research, Vol. 69, pp. 5181-5190

Shore Protection Manual 1984. US Army Engineer Waterway Experiment Station, Coastal Engineering Research Center (CERC), US Government Printing Office, Washington, D.C. , 4th edition, 2 Volumes

Smith D.S., Anderson J.R., Oost W.A., Kraan C., Maat N., DeCosmo J., Katsaros K.B., Davidson K.L., Bumke K., Hasse L., Chadwick H.M. 1992. Sea Surface Wind Stress and Drag Coefficients, The HEXOS Results, Boundary-Layer Meteorology, Vol. 60, pp. 109-142

Taylor P.A. and Lee R.J. 1984. Simple Guidelines for Estimating Wind Speed Variations due to Small Scale Topographic Features, Climatological Bulletin, Vol. 18, No. 2, pp. 3-32

Vincent C.L., Hughes S.T. 1985. Wind Wave Growth in Shallow Water, Journal of Waterway, Port, Coastal and Ocean Engineering, Vol. 111, No. 4, pp. 765-770

Wamdi Group 1988. The WAM Model- A Third Generation Ocean Wave Prediction Model, Journal of Physical Oceanography, Vol. 18, pp. 1775-1810

Wu J. 1980. Wind-Stress Coefficients over Sea Surface near Neutral Conditions-A Revisit, Journal of Physical Oceanography, Vol. 10 Part 1, pp 727-740

Young I.R.,1988, A shallow water spectral wave model, Journal of Geophysical Research, Vol. 93,C5, pp. 5113-5129

Young I.R., 1995, On the Measurement of Directional Wave Spectra, In press, Applied Ocean Research

Zwarts C.M.G. 1974. Transmission Line Wave Height Transducer, Proceedings International Symposium on Ocean Wave Measurement and Analysis, New Orleans, ASCE, Vol. 1, pp. 605-620